

<b>Statistica Sinica Preprint No: SS-2020-0334</b>	
<b>Title</b>	Quantification of model bias underlying the phenomenon of Einstein from Noise
<b>Manuscript ID</b>	SS-2020-0334
<b>URL</b>	<a href="http://www.stat.sinica.edu.tw/statistica/">http://www.stat.sinica.edu.tw/statistica/</a>
<b>DOI</b>	10.5705/ss.202020.0334
<b>Complete List of Authors</b>	Shao-Hsuan Wang, Yi-Ching Yao, Wei-Hau Chang and I-Ping Tu
<b>Corresponding Author</b>	I-Ping Tu
<b>E-mail</b>	iping@stat.sinica.edu.tw
Notice: Accepted version subject to English editing.	

## Quantification of model bias underlying the phenomenon of “Einstein from noise”

Shao-Hsuan Wang, Yi-Ching Yao, Wei-Hau Chang and I-Ping Tu

*Academia Sinica*

*Abstract:* Arising from cryogenic electron microscopy image analysis, “Einstein from noise” is a phenomenon of significant statistical interest because spurious patterns could easily emerge by averaging a large number of white-noise images aligned to a reference image through rotation and translation. While this phenomenon is often attributed to model bias, quantitative studies on such a bias are lacking. Here, we introduce a simple framework under which an image of  $p$  pixels is treated as a vector of dimension  $p$  and a white-noise image is a random vector uniformly sampled from the  $(p - 1)$ -dimensional unit sphere. Moreover, we adopt the cross correlation of two images which is a similarity measure based on the dot product of image pixels. This framework geometrically explains how the bias results from averaging a properly chosen set of white-noise images that are most highly cross-correlated with the reference image. We quantify the bias in terms of three parameters: the number of white-noise images ( $n$ ), the image dimension ( $p$ ), and the size of the selection set ( $m$ ). Under the conditions that  $n$ ,  $p$  and  $m$  are all large and  $(\ln n)^2/p$  and  $m/n$  are both small, we show that the bias is approximately  $\sqrt{\frac{2\gamma}{1+2\gamma}}$  where  $\gamma = \frac{m}{p} \ln \left( \frac{n}{m} \right)$ .

---

*Key words and phrases:* Cryogenic electron microscopy; cross correlation; extreme value distribution; model bias; high dimensional data analysis; white-noise image

## 1. Introduction

2 The terminology of the phenomenon of “Einstein from noise” comes from  
the literature of cryogenic electron microscopy (cryo-EM). It refers to an  
4 artefact of model bias that arises from averaging a large number of cryo-EM  
images aligned to a reference (model) image. This artefact of model bias is  
6 strongly associated with the noisy nature of cryo-EM images.

Developed for imaging biological macromolecules preserved at a frozen-  
8 hydrated state, cryo-EM has become a major tool for high-resolution struc-  
ture determination of molecules because of its recent breakthroughs in res-  
10 olution. In contrast to X-ray crystallography, cryo-EM does not need crys-  
tals, and thereby is amenable to structure determination of proteins that  
12 are refractory to crystallization, including, in particular, membrane pro-  
teins (Liao et al., 2013) and molecular complexes that exhibit dynamic  
14 conformation behaviors (Yan et al., 2015). To recognize its great success  
with far-reaching applications, the Nobel Prize in Chemistry in 2017 was  
16 awarded to J. Dubochet, J. Frank and R. Henderson for their pioneering

---

contributions to the development of cryo-EM.

18 A technical difficulty encountered by the cryo-EM technique is that dur-  
ing the experiment of imaging molecules, the orientation of each molecule is  
20 not recorded which needs to be estimated at the post-imaging stage. How-  
ever, to mitigate radiation damages, only a minimal dose of electron can be  
22 used for acquiring the projection images of individual molecules (called 2D  
particle images). The resulting cryo-EM images are extremely noisy with  
24 the signal-to-noise ratio less than 0.1. A typical cryo-EM experiment tends  
to collect a large number of particle images in hope of compensating the  
26 noise contamination by averaging, where the dimension of a particle image is  
extremely high (larger than one hundred by one hundred). Hence, the data  
28 characters of cryo-EM images, including strong noise contamination, huge  
dimension and large sample size, make its processing and statistical analysis  
30 very challenging. Henderson (2013) further pointed out how spurious pat-  
terns could easily emerge by averaging a large number of white-noise images  
32 aligned to a reference image through rotation and translation. Specifically,  
he referred to the work of Stewart and Grigorieff (2004) in which an exper-  
34 iment was conducted by generating 1000 white-noise images and aligning  
each of them to Einstein's facial image through rotation and translation.  
36 A blurred Einstein's face emerged from averaging the 1000 aligned images,

---

which Henderson (2013) dubbed “Einstein from noise” and used it to give  
 38 unwary cryo-EM users a warning that an incorrect 3D density map could  
 be constructed if data are blindly fitted to a reference model.

40 In a recent review paper, Lai et al. (2020) discussed the “Einstein from  
 noise” phenomenon from a statistical perspective. To avoid the technical  
 42 issue of how rotating an image may destroy the pixel format, they consid-  
 ered a simple mathematical framework under which an image of  $p$  pixels  
 44 is treated as a vector of dimension  $p$  and a white-noise image is a random  
 vector uniformly distributed on the  $(p - 1)$ -dimensional unit sphere. The  
 46 cross correlation of two images is adopted which is a similarity measure  
 based on the dot product of image pixels and is widely used in image pro-  
 48 cessing. Under this framework, we present in Section 2 a simulation study  
 with  $n = 2 \times 10^6$  white-noise images with the pixel number  $p = 120 \times 120$ .  
 50 Among the  $2 \times 10^6$  white-noise images, the largest cross correlation value  
 with Einstein’s facial image (the reference) is merely 0.039, while the cross  
 52 correlation increases dramatically to 0.650 after averaging the  $m = 800$  im-  
 ages that have the largest cross correlation values with Einstein’s facial im-  
 54 age. This illustrates the essence of the “Einstein from noise” phenomenon.  
 The objective of the present paper is to provide a thorough study of the  
 56 “Einstein from noise” phenomenon based on the statistical perspective laid

---

out in Lai et al. (2020). A main task is to approximate the distribution  
of the cross correlation between the (normalized) average of the  $m$  selected  
images and the reference, which is referred to the (image selection) bias.

While the bias depends on the three parameters  $n$ ,  $p$ , and  $m$  in a convoluted  
manner, under the conditions that  $n$ ,  $p$  and  $m$  are all large and  $(\ln n)^2/p$   
and  $m/n$  are both small, we show that the bias is approximately  $\sqrt{\frac{2\gamma}{1+2\gamma}}$   
where  $\gamma = \frac{m}{p} \ln \left( \frac{n}{m} \right)$ .

The rest of this paper is organized as follows. Section 2 introduces  
notation, terminology and the statistical model as well as demonstrates the  
phenomenon of “Einstein from noise”. Section 3 consists of two parts: (i)  
presenting an extreme value theory for the distribution of the largest cross  
correlation value as  $n$  and  $p$  both tend to infinity and (ii) stating asymptotic  
results on the bias as  $n$ ,  $p$ , and  $m$  all tend to infinity. The theoretical results  
in part (ii) are validated via simulation as presented in Section 4. Section 5  
contains concluding remarks. Proofs of the asymptotic results in Section 3  
are relegated to the Appendix. The online supplementary material contains  
the proofs of auxiliary lemmas.

---

## 2. Statistical Model

### 2.1 Notation, terminology, and model

Let  $\mathbf{R}$  be the reference matrix (the digital version of the reference image) of dimension  $d_1 \times d_2$ . We assume that  $\|\mathbf{R}\| = 1$  where  $\|\cdot\|$  denotes the Frobenius norm of a matrix or Euclidean norm of a vector. We generate  $n$  independent and identically distributed (iid) white-noise images as follows. Let  $\mathbf{Z}_1, \dots, \mathbf{Z}_n$  be iid  $d_1 \times d_2$  random matrices such that the  $d_1 d_2$  components of each  $\mathbf{Z}_i$  are iid standard normal. We refer to  $\mathbf{Z}_i / \|\mathbf{Z}_i\|$ ,  $i = 1, \dots, n$  (the normalized version of  $\mathbf{Z}_i$ ) as  $n$  iid white-noise images.

Let  $\mathbf{r} = \text{vec}(\mathbf{R})$ , the  $p$ -dimensional column vector which is the vectorized version of  $\mathbf{R}$ , where  $p = d_1 d_2$ . The fact that  $\|\mathbf{r}\| = 1$  implies  $\mathbf{r} \in \mathcal{S}^{p-1}$  (the  $(p-1)$ -dimensional unit sphere). Let  $\mathbf{X}_i = \text{vec}(\mathbf{Z}_i) / \|\mathbf{Z}_i\|$ . Thus,  $\mathbf{X}_1, \dots, \mathbf{X}_n$  are iid uniformly distributed on  $\mathcal{S}^{p-1}$ . We refer to both  $\mathbf{Z}_i / \|\mathbf{Z}_i\|$  and  $\mathbf{X}_i$  as the  $i$ -th white-noise image. With  $\mathbf{r}^\top$  denoting the transpose of  $\mathbf{r}$ , the cross correlation of  $\mathbf{X}_i$  and  $\mathbf{r}$  (or equivalently  $\mathbf{Z}_i / \|\mathbf{Z}_i\|$  and  $\mathbf{R}$ ) is defined as  $\mathbf{r}^\top \mathbf{X}_i$ , the inner product (dot product) of  $\mathbf{X}_i$  and  $\mathbf{r}$ , which is a similarity measure of two images. Note that  $\mathbf{r}^\top \mathbf{X}_i = \cos \Theta_i$ , where  $\Theta_i$  is the angle between  $\mathbf{r}$  and  $\mathbf{X}_i$ .

The  $n$  white-noise images are ordered (and denoted by  $\mathbf{X}^{(1)}, \dots, \mathbf{X}^{(n)}$ )

## 2.2 Demonstration of the “Einstein from noise” phenomenon

according to their cross correlation values with  $\mathbf{r}$ . In other words,  $(\mathbf{X}^{(1)}, \dots, \mathbf{X}^{(n)})$

94 is a permutation of  $(\mathbf{X}_1, \dots, \mathbf{X}_n)$  such that  $\mathbf{r}^\top \mathbf{X}^{(1)} \geq \mathbf{r}^\top \mathbf{X}^{(2)} \geq \dots \geq \mathbf{r}^\top \mathbf{X}^{(n)}$ .

Let  $\Theta_{1:n} \leq \Theta_{2:n} \leq \dots \leq \Theta_{n:n}$  be the order statistics of the angles  $(\Theta_1, \dots, \Theta_n)$ ,

96 so that  $\cos \Theta_{i:n} = \mathbf{r}^\top \mathbf{X}^{(i)}$ ,  $i = 1, \dots, n$ . Let  $\bar{\mathbf{X}}_m = m^{-1} \sum_{i=1}^m \mathbf{X}^{(i)}$ . Then

$\bar{\mathbf{X}}_m / \|\bar{\mathbf{X}}_m\| \in \mathcal{S}^{p-1}$  is the normalized average of the  $m$  white-noise images

98 that are most highly cross-correlated with the reference image. Our goal is

to find a good approximation of the distribution of  $\rho_{n,p,m} = \mathbf{r}^\top \bar{\mathbf{X}}_m / \|\bar{\mathbf{X}}_m\|$

100 when  $n$ ,  $p$ , and  $m$  are large. Note that for  $m = 1$ ,  $\rho_{n,p,1} = \mathbf{r}^\top \mathbf{X}^{(1)} = \cos \Theta_{1:n}$ ,

is the largest cross correlation value. Note also that the distribution of

102  $\rho_{n,p,m}$  does not depend on  $\mathbf{r}$  which is due to the fact that if  $\mathbf{X}$  is uniformly

distributed on  $\mathcal{S}^{p-1}$ , then the distribution of  $\mathbf{r}^\top \mathbf{X}$  is independent of  $\mathbf{r}$ .

## 104 2.2 Demonstration of the “Einstein from noise” phenomenon

We now present two figures summarizing the simulation study described

106 in Section 1, where  $n = 2 \times 10^6$ ,  $p = d_1 \times d_2 = 120 \times 120 = 14400$ , and

$m = 1, 200, 400, 800$ . In Figure 1, the leftmost (reference) image is Ein-

108 stein’s face, and the other 4 images correspond to  $\bar{\mathbf{X}}_m / \|\bar{\mathbf{X}}_m\|$  for  $m =$

1, 200, 400, 800. The second image from the left corresponds to  $\mathbf{X}^{(1)}$ , whose

110 cross correlation (CC) value with Einstein’s facial image is 0.039 (which is

the largest among the  $2 \times 10^6$  white-noise images generated in the simula-



## 2.2 Demonstration of the “Einstein from noise” phenomenon

tion). While this image is rather noisy, Einstein’s face emerges in the other  
3 images with different degrees of blurring, corresponding to CC values  
0.426, 0.536, and 0.650.

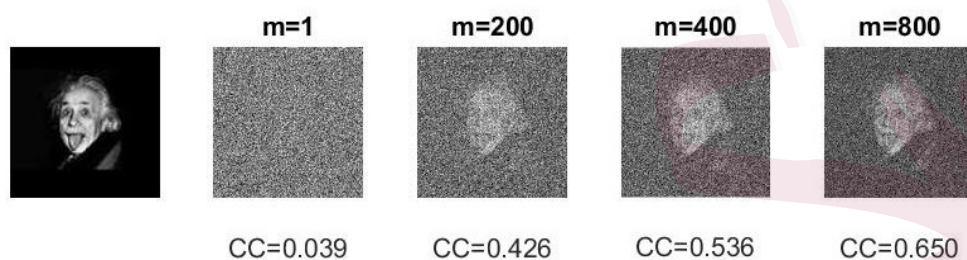


Figure 1: Example with Einstein’s face as the reference image.

## 2.2 Demonstration of the “Einstein from noise” phenomenon

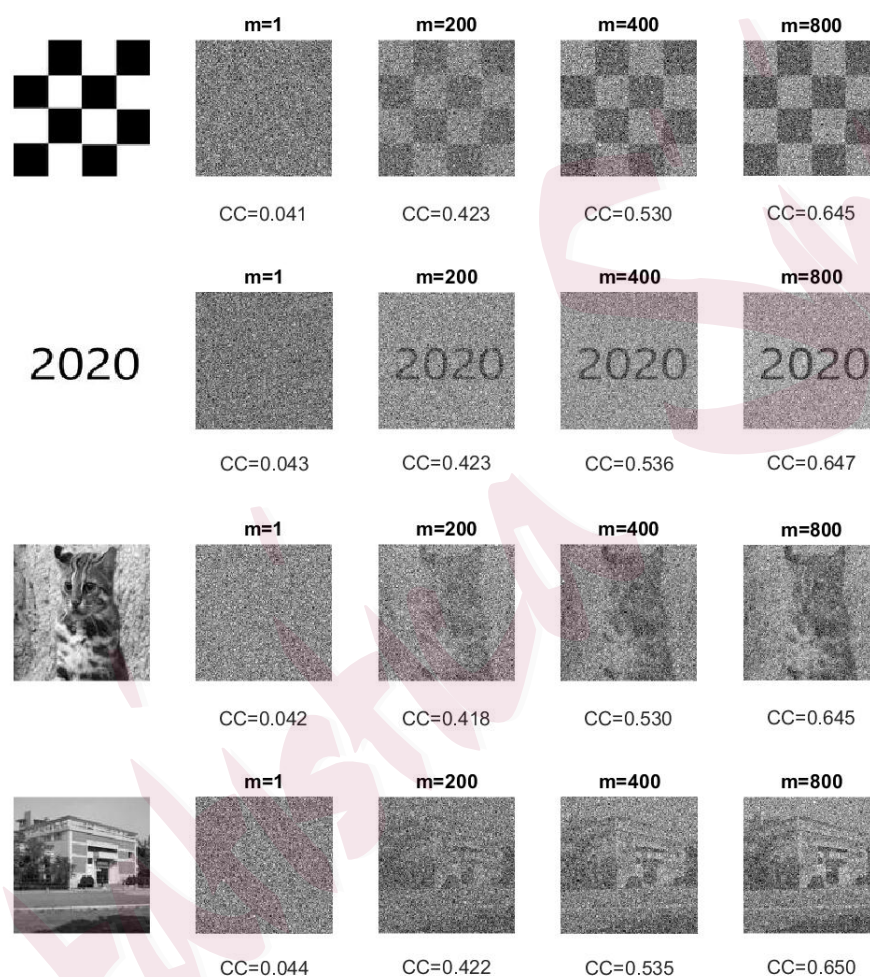


Figure 2: The phenomenon of “Einstein from noise” is shown across various reference images.

---

Figure 2 shows similar results with four different reference images of a  
 116 simple chessboard, digits of 2020, a leopard cat and Statistics Building of  
 Academia Sinica, indicating that the phenomenon of “Einstein from noise”  
 118 is robust across various reference images. The cross correlation values in  
 Figure 2 are about the same across different reference images, which can  
 120 be explained by the previously mentioned fact that if  $\mathbf{X}$  is uniformly dis-  
 tributed on  $\mathcal{S}^{p-1}$ , then the distribution of  $\mathbf{r}^\top \mathbf{X}$  is independent of  $\mathbf{r}$ .

122

### 3. Asymptotic theory

#### 124 3.1 Extreme value theory for the largest cross correlation

Recall that  $\cos \Theta_{1:n}$  is the largest cross correlation. The following theorem  
 126 provides an approximation to the distribution of  $\cos \Theta_{1:n}$  when  $n$  and  $p$  are  
 large.

128 **Theorem 1.** *Let*

$$K_{n,p} = -\ln n + \frac{1}{2} \ln \ln n - \frac{1}{2} \ln \left( \frac{2^{\frac{\ln n}{p}}}{1 - \exp \left( -2^{\frac{\ln n}{p}} \right)} \right) + \frac{1}{2} \ln(4\pi). \quad (1)$$

*We have*

$$(p-1) \ln(\sin \Theta_{1:n}) - K_{n,p} \xrightarrow{d} G \text{ uniformly as } n \wedge p \rightarrow \infty, \quad (2)$$

### 3.1 Extreme value theory for the largest cross correlation

130 where  $n \wedge p = \min\{n, p\}$ ,  $\xrightarrow{d}$  denotes convergence in distribution, and the  
cumulative distribution function of  $G$  is given by  $G(t) = 1 - e^{-e^t}$ ,  $t \in \mathbb{R}$ ,  
132 which is known as the extreme value distribution of Gumbel type.

Based on (2), for  $0 < \alpha < 1$ , the approximate  $100\alpha$ -th quantile of the  
distribution of  $\cos \Theta_{1:n}$  is

$$M_{n,p}(\alpha) = \sqrt{1 - \exp\{2(K_{n,p} + \ln \ln \alpha^{-1})/(p-1)\}}.$$

Recall that  $\cos \Theta_{1:n} = 0.039$  in the simulation study summarized in Figure  
134 1, where  $n = 2 \times 10^6$  and  $p = 120 \times 120$ . This observed value is compatible  
with the approximate 10th quantile  $M_{n,p}(0.1) = 0.039$ .

136 Figure 3 plots  $M_{n,p}(\alpha)$  versus  $\log_{10} n$  for  $n \leq 10^{100}$  with  $p = 120 \times 120$   
and  $\alpha = .05, .5, .95$ . Note that the three quantile curves are very close to  
138 each other, indicating that  $\cos \Theta_{1:n}$  has a small standard deviation. Figure  
3 suggests that for  $P(\cos \Theta_{1:n} \geq 0.1)$  to be at least 0.05,  $n$  is required to  
140 be greater than  $10^{30}$ , and for  $P(\cos \Theta_{1:n} \geq 0.15)$  to be at least 0.05,  $n$  is  
required to be greater than  $10^{70}$ . In other words, it is unlikely for any of  
142  $n$  iid white-noise images of dimension  $120 \times 120$  to have a cross correlation  
value with Einstein's face greater than 0.15 unless  $n$  is astronomically large.

### 3.2 Asymptotic results on $\rho_{n,p,m}$

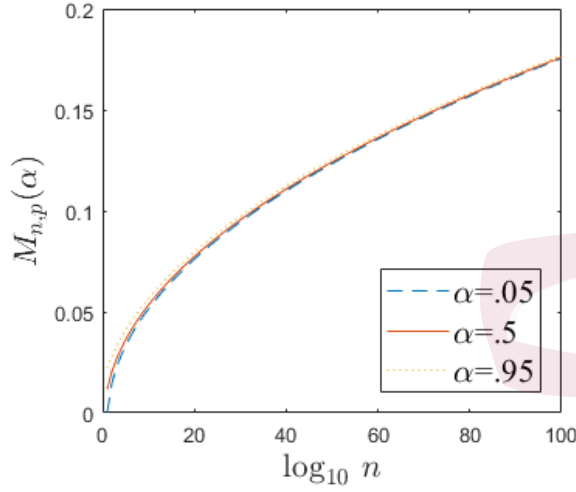


Figure 3: The approximate  $100\alpha$ -th quantile of the distribution of  $\cos \Theta_{1:n}$  ( $M_{n,p}(\alpha)$ ) versus  $\log_{10} n$  with  $p = 120 \times 120$ ,  $\alpha = .05, .5, .95$ .

### 144 3.2 Asymptotic results on $\rho_{n,p,m}$

When  $p = p_n$  and  $m = m_n$  both grow with  $n$ , asymptotic expansions for the distribution of  $\rho_{n,p,m}$  are more involved. Our analysis requires the condition  $(\ln n)^2/p = o(1)$  (which is stronger than  $(\ln n)/p = o(1)$ ), so that terms such as  $(\ln n)(\ln \ln n)/p$  become negligible. Let

$$\beta_{n,p,m} = \frac{m}{p} \left\{ 2 \ln \frac{n}{m} - \ln \ln \frac{n}{m} - \ln(4\pi) + 2 \right\},$$

which is a model bias index. While the quantity  $\rho_{n,p,m}$  plays an important role in our asymptotic results below, we are unaware of any heuristic interpretation of this quantity.

### 3.2 Asymptotic results on $\rho_{n,p,m}$

**Theorem 2.** Let  $p = p_n \rightarrow \infty$  satisfy  $(\ln n)^2/p = o(1)$  and  $m = m_n \rightarrow \infty$  satisfy  $m/n = o(1)$ . Then

$$\rho_{n,p,m}^2 = \frac{\beta_{n,p,m}}{1 + \beta_{n,p,m}} (1 + o_p(1)).$$

Consequently,  $\rho_{n,p,m}^2 - \frac{\beta_{n,p,m}}{1 + \beta_{n,p,m}} \rightarrow 0$  in probability.

**Theorem 3.** Let  $p = p_n \rightarrow \infty$  satisfy  $(\ln n)^2/p = o(1)$  and  $m = m_n \rightarrow \infty$  satisfy  $m(\ln \ln n)^4/(\ln n)^2 = o(1)$ . Then

$$\alpha_{n,p,m} \left( \rho_{n,p,m}^2 - \frac{\beta_{n,p,m}}{1 + \beta_{n,p,m}} \right) \xrightarrow{d} N(0, 1),$$

where  $\alpha_{n,p,m} = p (8m + 2p \beta_{n,p,m}^2)^{-1/2} (1 + \beta_{n,p,m})^2$  and  $N(0, 1)$  denotes the standard normal distribution.

**Corollary 1.** Let  $p = p_n \rightarrow \infty$  and  $m = m_n \rightarrow \infty$ .

(i) If  $(\ln n)^2/p = o(1)$  and  $m/n = o(1)$ , then

$$\frac{\rho_{n,p,m}}{\sqrt{\beta_{n,p,m}/(1 + \beta_{n,p,m})}} = 1 + o_p(1).$$

Consequently,

$$\rho_{n,p,m} = \sqrt{\frac{\beta_{n,p,m}}{1 + \beta_{n,p,m}}} + o_p(1) \quad \text{and} \quad E(\rho_{n,p,m}) = \sqrt{\frac{\beta_{n,p,m}}{1 + \beta_{n,p,m}}} + o(1).$$

(ii) In addition to the conditions specified in (i), if  $m(\ln \ln n)^4/(\ln n)^2 = o(1)$ , then

$$\tilde{\alpha}_{n,p,m} \left( \rho_{n,p,m} - \sqrt{\frac{\beta_{n,p,m}}{1 + \beta_{n,p,m}}} \right) \xrightarrow{d} N(0, 1),$$

### 3.2 Asymptotic results on $\rho_{n,p,m}$

where  $\tilde{\alpha}_{n,p,m} = 2\alpha_{n,p,m}\sqrt{\beta_{n,p,m}/(1 + \beta_{n,p,m})}$ .

**Remark 1.** On top of the condition  $(\ln n)^2/p = o(1)$ , Theorem 2 only requires the mild condition  $m/n = o(1)$ . Let  $\gamma_{n,p,m} = \frac{m}{p} \ln \frac{n}{m}$ . Since  $\beta_{n,p,m} = 2\gamma_{n,p,m}(1+o(1))$  (i.e.  $2\gamma_{n,p,m}$  is the leading term of  $\beta_{n,p,m}$ ), Theorem 2 implies

$$\rho_{n,p,m}^2 = \frac{2\gamma_{n,p,m}}{1 + 2\gamma_{n,p,m}} + o_p(1).$$

Consequently,

$$\rho_{n,p,m} = \sqrt{\frac{2\gamma_{n,p,m}}{1+2\gamma_{n,p,m}}} + o_p(1) \quad \text{and} \quad E(\rho_{n,p,m}) = \sqrt{\frac{2\gamma_{n,p,m}}{1+2\gamma_{n,p,m}}} + o(1). \quad (3)$$

**Remark 2.** To establish asymptotic normality of  $\rho_{n,p,m}^2$  (and  $\rho_{n,p,m}$ ), Theorem 3 (and Corollary 1) requires the stringent condition  $m(\ln \ln n)^4/(\ln n)^2 = o(1)$ . It is unclear whether asymptotic normality still holds when  $m$  grows at a rate faster than  $(\ln n)^2/(\ln \ln n)^4$ . It should also be remarked that under the conditions as in Theorem 3, it is not true that  $\alpha_{n,p,m} \left( \rho_{n,p,m}^2 - \frac{2\gamma_{n,p,m}}{1+2\gamma_{n,p,m}} \right) \xrightarrow{d} N(0, 1)$ . This shows that while  $2\gamma_{n,p,m}$  is the leading term of  $\beta_{n,p,m}$ , the remaining terms also play a non-negligible role in the proof of asymptotic normality.

**Remark 3.** Fan et al. (2018) developed an asymptotic theory to approximate the distribution of the maximum spurious correlation of a response variable  $Y$  with the best  $m$  linear combinations of  $p$  covariates  $\mathbf{X}$  based

---

174 on an iid sample of size  $n$  when  $\mathbf{X}$  and  $Y$  are independent. See also Fan  
et al. (2012) for related results. In our setting, the quantity  $\rho_{n,p,m}$  may  
176 be referred to as the spurious cross correlation of the reference with the  
normalized average of the  $m$  white-noise images that are most highly cross-  
178 correlated with the reference. Indeed, with the roles of  $n$  and  $p$  reversed,  
 $\rho_{n,p,m}$  corresponds to another spurious correlation of the response variable  
180  $Y$  with the the average of the  $m$  (standardized) covariates in  $\mathbf{X}$  that are  
most highly correlated with  $Y$  when the  $p$  covariates in  $\mathbf{X}$  and  $Y$  are all  
182 mutually independent.

#### 4. Simulation Results on $\rho_{n,p,m}$

184 By Corollary 1(i), if  $m$  is small compared to  $n$  and  $(\ln n)^2$  is small compared  
to  $p$ , then  $E(\rho_{n,p,m})$  is expected to be close to  $\sqrt{\frac{\beta_{n,p,m}}{1+\beta_{n,p,m}}}$  while the standard  
186 deviation (s.d.) of  $\rho_{n,p,m}$  is expected to be small. We conducted a simulation  
study of the distribution of  $\rho_{n,p,m}$  for various combinations of  $(n, p, m)$  with  
188  $n = 10^4, 10^5$ ,  $p = 10^4, 4 \times 10^4$ , and  $m = 100, 200, 400, 600$ . The results are  
reported in Tables 1 and 2 where  $E(\rho_{n,p,m})$  and  $\text{s.d.}(\rho_{n,p,m})$  were estimated  
190 based on 1000 replications for each case. While  $\sqrt{\frac{\beta_{n,p,m}}{1+\beta_{n,p,m}}}$  approximates  
 $E(\rho_{n,p,m})$  well, it slightly overestimates  $E(\rho_{n,p,m})$ , more notably for  $n = 10^4$ .  
192 Clearly,  $E(\rho_{n,p,m})$  increases as  $n$  or  $m$  increases or  $p$  decreases. On the



---

other hand,  $\text{s.d.}(\rho_{n,p,m})$  is small ( $< .005$ ) in all cases. Besides,  $\text{s.d.}(\rho_{n,p,m})$   
 194 decreases as  $n$  or  $p$  increases, and is about the same as  $m$  varies from 100 to  
 600. Also included in Tables 1 and 2 are  $\tilde{\alpha}_{n,p,m}^{-1}$  and the empirical probability  
 196 (denoted as Prob.) that

$$\left| \rho_{n,p,m} - \sqrt{\frac{\beta_{n,p,m}}{1 + \beta_{n,p,m}}} \right| < 1.96 \tilde{\alpha}_{n,p,m}^{-1}.$$

It is clear from the tables that  $\tilde{\alpha}_{n,p,m}^{-1}$  approximates  $\text{s.d.}(\rho_{n,p,m})$  reasonably  
 198 well in all cases. By Corollary 1(ii), the Prob. value is expected to be  
 close to .95 if the normal approximation is accurate. By Theorem 3 and  
 200 Corollary 1,  $\alpha_{n,p,m} \left( \rho_{n,p,m}^2 - \frac{\beta_{n,p,m}}{1 + \beta_{n,p,m}} \right)$  and  $\tilde{\alpha}_{n,p,m} \left( \rho_{n,p,m} - \sqrt{\frac{\beta_{n,p,m}}{1 + \beta_{n,p,m}}} \right)$  are  
 approximately standard normal under somewhat stringent conditions on  
 202 the growth rates of  $m$  and  $p$  as  $n \rightarrow \infty$ . While none of the combinations  
 of  $(n, p, m)$  with  $n = 10^4, 10^5$ ,  $p = 10^4, 4 \times 10^4$  and  $m = 100, 200, 400, 600$   
 204 seems to satisfy the condition that  $m (\ln \ln n)^4 / (\ln n)^2$  be small, the normal  
 approximation appears to be acceptable for  $n = 10^5$  but less satisfactory  
 206 for  $n = 10^4$ .

Table 1:  $p = 10^4$ .

$m$	$n = 10^4$				$n = 10^5$			
	100	200	400	600	100	200	400	600
$E(\rho_{n,p,m})$	0.257	0.323	0.395	0.437	0.318	0.408	0.509	0.570
$\sqrt{\frac{\beta_{n,p,m}}{1+\beta_{n,p,m}}}$	0.258	0.325	0.399	0.442	0.319	0.409	0.510	0.571
$\text{s.d.}(\rho_{n,p,m})$	0.0043	0.0045	0.0046	0.0048	0.0039	0.0039	0.0040	0.0037
$\tilde{\alpha}_{n,p,m}^{-1}$	0.0051	0.0053	0.0055	0.0057	0.0041	0.0042	0.0040	0.0039
Prob.	0.974	0.967	0.942	0.870	0.967	0.959	0.947	0.953

Table 2:  $p = 4 \times 10^4$ .

$m$	$n = 10^4$				$n = 10^5$			
	100	200	400	600	100	200	400	600
$E(\rho_{n,p,m})$	0.132	0.168	0.210	0.236	0.165	0.218	0.283	0.327
$\sqrt{\frac{\beta_{n,p,m}}{1+\beta_{n,p,m}}}$	0.132	0.169	0.212	0.239	0.166	0.219	0.284	0.328
$\text{s.d.}(\rho_{n,p,m})$	0.0022	0.0024	0.0026	0.0027	0.0019	0.0020	0.0021	0.0022
$\tilde{\alpha}_{n,p,m}^{-1}$	0.0026	0.0028	0.0031	0.0033	0.0021	0.0022	0.0023	0.0023
Prob.	0.977	0.978	0.946	0.871	0.968	0.967	0.955	0.953

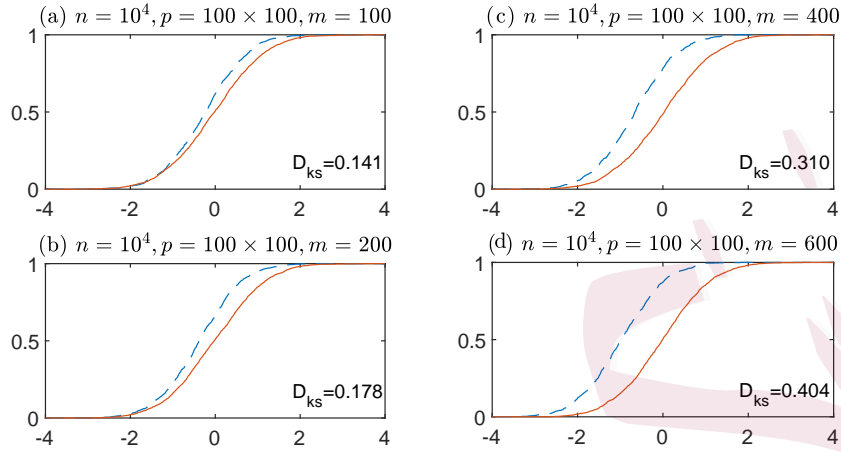


Figure 4: Empirical cdf of  $\tilde{\alpha}_{n,p,m}(\rho_{n,p,m} - \sqrt{\beta_{n,p,m}/(1 + \beta_{n,p,m})})$  (dashed curves) and standard normal cdf (solid curves):  $n = 10^4$ ,  $p = 10^4$ .

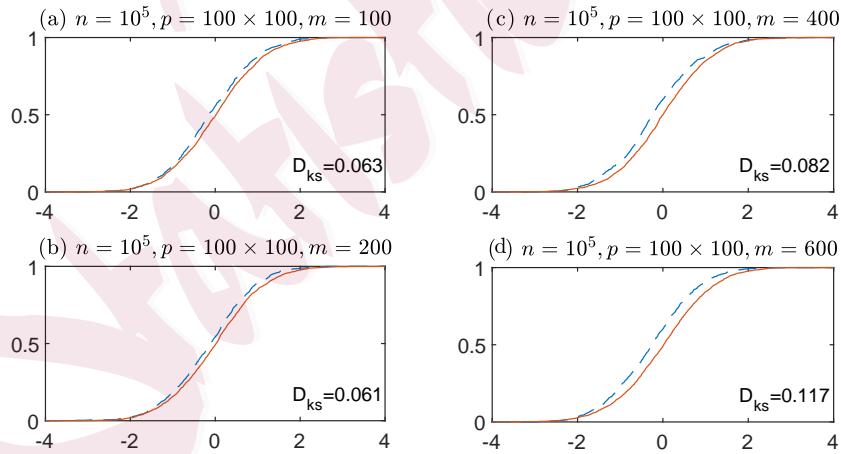


Figure 5: Empirical cdf of  $\tilde{\alpha}_{n,p,m}(\rho_{n,p,m} - \sqrt{\beta_{n,p,m}/(1 + \beta_{n,p,m})})$  (dashed curves) and standard normal cdf (solid curves):  $n = 10^5$ ,  $p = 10^4$ .

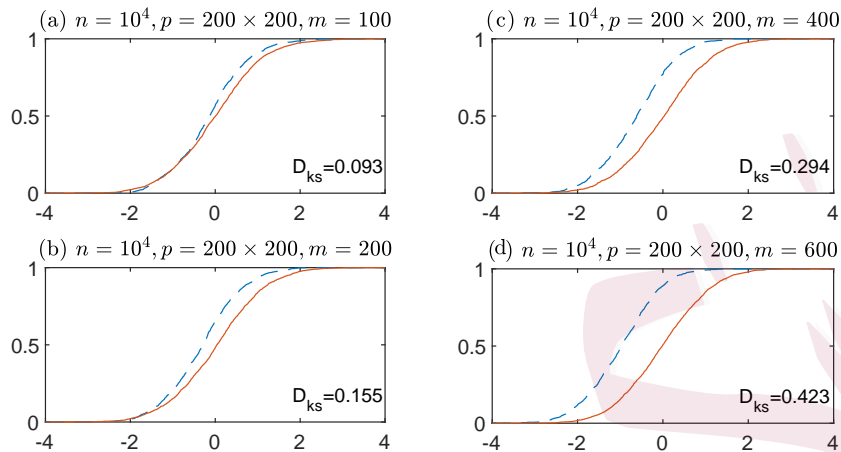


Figure 6: Empirical cdf of  $\tilde{\alpha}_{n,p,m}(\rho_{n,p,m} - \sqrt{\beta_{n,p,m}/(1 + \beta_{n,p,m})})$  (dashed curves) and standard normal cdf (solid curves):  $n = 10^4$ ,  $p = 4 \times 10^4$ .

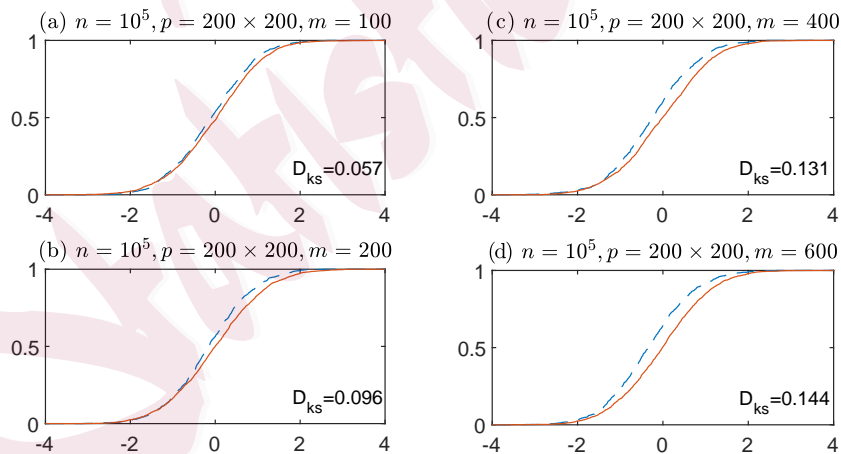


Figure 7: Empirical cdf of  $\tilde{\alpha}_{n,p,m}(\rho_{n,p,m} - \sqrt{\beta_{n,p,m}/(1 + \beta_{n,p,m})})$  (dashed curves) and standard normal cdf (solid curves):  $n = 10^5$ ,  $p = 4 \times 10^4$ .

---

To get a more complete picture of the quality of the normal approximation in Corollary 1(ii), in Figures 4-7, we plot the empirical cumulative distribution function (cdf) of  $\tilde{\alpha}_{n,p,m} \left( \rho_{n,p,m} - \sqrt{\frac{\beta_{n,p,m}}{1+\beta_{n,p,m}}} \right)$  (based on 1000 replications), along with the standard normal cdf for each combination of  $(n, p, m)$ . (The value of  $D_{ks}$  is the Kolmogorov-Smirnov distance between the two cdfs.) Figures 4-7 are the cdf under four different scenarios, depending on the values of  $n = 10^4, 10^5$  and  $p = 10^4, 4 \times 10^4$ . In each figure, it includes four plots, depending on the values of  $m = 100, 200, 400, 600$ . The empirical cdf is shifted to the left of the standard normal cdf (more notably for  $n = 10^4$  in Figures 4 and 6), indicating that the mean of  $\rho_{n,p,m} - \sqrt{\frac{\beta_{n,p,m}}{1+\beta_{n,p,m}}}$  is negative. This is consistent with the results in Tables 1 and 2 where  $\sqrt{\frac{\beta_{n,p,m}}{1+\beta_{n,p,m}}}$  (slightly) overestimates  $E(\rho_{n,p,m})$  (more notably for  $n = 10^4$ ).

## 5. Concluding Remarks

This paper studied a simple statistical model in order to quantitatively examine the phenomenon of “Einstein from noise”. Specifically, for a given reference image of dimension  $p$  and a set  $S_n$  of  $n$  iid white-noise images (with the common uniform distribution on  $\mathcal{S}^{p-1}$ ), we derived the asymptotic behavior of the cross correlation  $\rho_{n,p,m}$  between the reference and the

---

226 normalized average of the  $m$  “most biased” members in  $S_n$  in the sense  
that they have the largest cross correlation values with the reference. Our  
228 theoretical results indicate that for  $m = 1$  and  $p = 120 \times 120$ , unless  $n$  is far  
beyond the practical range ( $> 10^{70}$ ),  $\rho_{n,p,1}$  is small ( $< 0.15$ ) with high prob-  
230 ability, implying that none of  $n$  white-noise images even remotely resembles  
the reference. On the other hand, for  $m$  moderately large ( $\geq 400$ ),  $\rho_{n,p,m}$   
232 exceeds 0.5 with high probability if  $n = 2 \times 10^6$ , in which case a blurred  
version of the reference emerges from the normalized average of the  $m$  most  
234 biased members in  $S_n$ .

Given a set  $S_n$  of  $n$  iid white-noise images, Cai et al. (2013) derived the  
236 asymptotic distribution of the maximum of all pairwise cross correlations  
in  $S_n$ . See also Cai and Jiang (2011, 2012) and references therein. In  
238 the absence of a reference image, their results may be applied to test the  
null hypothesis that  $S_n$  consists of  $n$  iid white-noise images. On the other  
240 hand, given a reference image, our results can be used to test such a null  
hypothesis against the alternative that some of the  $n$  images in  $S_n$  are biased  
242 towards the reference by checking whether  $\rho_{n,p,m}$  exceeds a threshold (which  
is determined by the null distribution of  $\rho_{n,p,m}$ ).

244 Our approach can be directly generalized to tackle a special case of  
multiple references. Let  $\mathbf{r}^{(1)}, \dots, \mathbf{r}^{(k)}$  be  $k$  given references of dimension

---

246  $p$ . Given a set  $S_n$  of  $n$  iid white-noise images, for  $i = 1, \dots, k$ , let  $\rho_{n,p,m}^{(i)}$   
 $(i = 1, \dots, k)$  denote the cross correlation between  $\mathbf{r}^{(i)}$  and the normal-  
248 ized average of those  $m$  members in  $S_n$  having the largest cross correlation  
values with  $\mathbf{r}^{(i)}$ . It would be of interest to derive the asymptotic distri-  
250 bution of  $\max\{\rho_{n,p,m}^{(i)} : i = 1, \dots, k\}$ . If  $\mathbf{r}^{(1)}, \dots, \mathbf{r}^{(k)}$  are orthogonal (i.e.  
the pairwise cross correlations are all equal to 0), then it can be argued  
252 that  $\rho_{n,p,m}^{(1)}, \dots, \rho_{n,p,m}^{(k)}$  are asymptotically independent, so that the asymp-  
totic distribution of  $\max\{\rho_{n,p,m}^{(i)} : i = 1, \dots, k\}$  can be readily derived by  
254 Corollary 1. However, it seems difficult to find the asymptotic distribution  
of  $\max\{\rho_{n,p,m}^{(i)} : i = 1, \dots, k\}$  when  $\mathbf{r}^{(1)}, \dots, \mathbf{r}^{(k)}$  are not orthogonal.

256 The phenomenon of “Einstein from noise” originally arose in the con-  
text of cryo-EM image analysis where a key component is image alignment  
258 (including rotation and translation). While to address this more compli-  
cated problem is beyond the scope of the present paper, it is worth noting  
260 that the geometric shape of the reference is likely to play a significant role  
in the asymptotic theory yet to be developed. As an example, consider a  
262 rotationally invariant reference, e.g. an image of a centered wheel. Because  
of rotational symmetry of the reference, a data image cannot fit the refer-  
264 ence any better by rotation. We leave this challenging problem for future  
work.

---

## Supplementary Material

The online Supplementary Material contains the proofs of Lemmas A6-A8 stated in the Appendix.

## Acknowledgements

The authors gratefully acknowledge support by Academia Sinica grant AS-GCS-108-08 and Taiwan's Ministry of Science and Technology grant 106-2118-M-001-001-MY2.

## A. Appendix

The Appendix consists of three sections. Section A.1 states some auxiliary lemmas, Section A.2 contains the proof of Theorem 1, and Section A.3 provides the proofs of Theorems 2 and 3 and Corollary 1. For easy reference, a complete list of notations is given in Supplementary Material. Note that if  $\mathbf{X}$  is uniformly distributed on  $\mathcal{S}^{p-1}$ , then the distribution of  $\mathbf{r}^\top \mathbf{X}$  is the same for all  $\mathbf{r} \in \mathcal{S}^{p-1}$ . Without loss of generality, we assume  $\mathbf{r} = (1, 0, \dots, 0)^\top \in \mathcal{S}^{p-1}$  in what follows.



### A.1. Auxiliary lemmas

282 **Lemma A1.** (Lemma 6.2 of Cai and Jiang (2012)) For  $t \in (0, 1)$ , we have

$$\left(1 + \frac{1}{pt^2}\right)^{-1} \frac{1}{(p+2)t} (1-t^2)^{(p+2)/2} \leq \int_t^1 (1-u^2)^{p/2} du \leq \frac{1}{(p+2)t} (1-t^2)^{(p+2)/2}.$$

Since  $\mathbf{X}_i$ ,  $i = 1, \dots, n$  are iid uniformly distributed on  $\mathcal{S}^{p-1}$  and  $\Theta_i$   
284 denotes the angle between  $\mathbf{X}_i$  and  $\mathbf{r} = (1, 0, \dots, 0)^\top$ , we have (cf. Eq (5)  
of Cai et al. (2013)) that  $\Theta_i$ ,  $i = 1, \dots, n$  are iid with the common cdf

$$\begin{aligned} F_p(\theta) &= \int_0^\theta \frac{1}{\sqrt{\pi}} \frac{\Gamma(p/2)}{\Gamma((p-1)/2)} (\sin x)^{p-2} dx \\ &= \int_{\cos \theta}^1 \frac{1}{\sqrt{\pi}} \frac{\Gamma(p/2)}{\Gamma((p-1)/2)} (1-u^2)^{\frac{p-3}{2}} du, \quad \theta \in [0, \pi]. \end{aligned} \quad (\text{A.1})$$

286 Let

$$\bar{F}_p(\theta) = \frac{1}{\sqrt{\pi}} \frac{\Gamma(p/2)}{\Gamma((p-1)/2)} \frac{\sin^{p-1} \theta}{(p-1)|\cos \theta|}. \quad (\text{A.2})$$

The following lemma is a consequence of Lemma A1.

**Lemma A2.** For  $\theta \in (0, \pi/2)$  and  $p > 3$ , we have

$$\left(1 + \frac{1}{(p-3)\cos^2 \theta}\right)^{-1} \bar{F}_p(\theta) \leq F_p(\theta) \leq \bar{F}_p(\theta).$$

288 Let  $U_1, U_2, \dots$  be iid uniform  $(0, 1)$  random variables and let  $U_{1:n} \leq$   
 $\dots \leq U_{n,n}$  denote the order statistics of  $U_1, \dots, U_n$ . Let  $S_0 = 0$ , and  
290  $S_i = \xi_1 + \dots + \xi_i$ ,  $i = 1, 2, \dots$ , where  $\xi_1, \xi_2, \dots$  are iid exponential random

variables with mean 1. The next lemma is well known; see e.g. Karlin and  
Taylor (1975). We write  $\mathbf{X} \stackrel{d}{=} \mathbf{Y}$  if random vectors  $\mathbf{X}$  and  $\mathbf{Y}$  are equal in  
distribution.

**Lemma A3.** (i)  $(U_{1:n}, \dots, U_{n:n}) \stackrel{d}{=} (S_1, \dots, S_n)/S_{n+1}$ . (ii)  $(S_1, \dots, S_n)/S_{n+1}$   
is independent of  $S_{n+1}$ .

Recall that  $(\mathbf{X}^{(1)}, \dots, \mathbf{X}^{(n)})$  is a permutation of  $(\mathbf{X}_1, \dots, \mathbf{X}_n)$  such  
that  $X_1^{(1)} \leq \dots \leq X_1^{(n)}$ , where  $X_1^{(i)} = \mathbf{r}^\top \mathbf{X}^{(i)}$  (the first component of  
 $\mathbf{X}^{(i)}$ ). Let  $\mathbf{V}_i$  and  $\mathbf{V}^{(i)}$  be defined by  $\mathbf{X}_i = (X_{i1}, (1 - X_{i1}^2)^{1/2} \mathbf{V}_i^\top)^\top$  and  
 $\mathbf{X}^{(i)} = (X_1^{(i)}, \nu_i \mathbf{V}^{(i)\top})^\top$ , where  $\nu_i = (1 - X_1^{(i)2})^{1/2}$ . In other words,  $\mathbf{V}_i$  ( $\mathbf{V}^{(i)}$ ,  
respectively)  $\in \mathcal{S}^{p-2}$  is the normalized subvector of  $\mathbf{X}_i$  ( $\mathbf{X}^{(i)}$ , respectively)  
with the first component deleted.

**Lemma A4.**

(i)  $X_{i1}$  and  $\mathbf{V}_i, i = 1, \dots, n$  are all independent.

(ii)  $X_{i1}, i = 1, \dots, n$  are iid.

(iii)  $\mathbf{V}_i, i = 1, \dots, n$  are iid with the uniform distribution on  $\mathcal{S}^{p-2}$ .

(iv)  $(\mathbf{V}^{(1)}, \dots, \mathbf{V}^{(n)})$  is independent of  $(X_{11}, \dots, X_{n1})$  and hence indepen-  
dent of  $(X_1^{(1)}, \dots, X_1^{(n)})$ .

(v)  $\mathbf{V}^{(i)}, i = 1, \dots, n$  are iid with the uniform distribution on  $\mathcal{S}^{p-2}$ .

To show Lemma A4, let  $Z_{ij}, i = 1, \dots, n, j = 1, \dots, p$ , be iid standard

normal, and let

$$\mathbf{X}_i^* = (Z_{i1}, \dots, Z_{ip})^\top / \sqrt{\sum_{j=1}^p Z_{ij}^2} = (Z_{i1} / \sqrt{\sum_{j=1}^p Z_{ij}^2}, \nu_i^* \mathbf{V}_i^*)^\top, \quad i = 1, \dots, n,$$

$$\text{where } \nu_i^* = \sqrt{\sum_{j=2}^p Z_{ij}^2} / \sqrt{\sum_{j=1}^p Z_{ij}^2} \text{ and } \mathbf{V}_i^* = (Z_{i2}, \dots, Z_{ip})^\top / \sqrt{\sum_{j=2}^p Z_{ij}^2}.$$

It is readily seen that  $\mathbf{X}_i^*$  is uniformly distributed on  $\mathcal{S}^{p-1}$  and independent of  $\sum_{j=1}^p Z_{ij}^2$ , and that  $\mathbf{V}_i^*$  is uniformly distributed on  $\mathcal{S}^{p-2}$  and independent of  $Z_{i1}$  and  $\sum_{j=2}^p Z_{ij}^2$  (hence independent of  $Z_{i1} / \sqrt{\sum_{j=1}^p Z_{ij}^2}$ ). Since  $(\mathbf{X}_1, \dots, \mathbf{X}_n) \stackrel{d}{=} (\mathbf{X}_1^*, \dots, \mathbf{X}_n^*)$  and  $(\mathbf{V}_1, \dots, \mathbf{V}_n) \stackrel{d}{=} (\mathbf{V}_1^*, \dots, \mathbf{V}_n^*)$ , Lemma A4 follows.

Recall that

$$\bar{\mathbf{X}}_m = \frac{1}{m} \sum_{i=1}^m \mathbf{X}^{(i)} = (m^{-1} \sum_{i=1}^m X_1^{(i)}, m^{-1} \sum_{i=1}^m \nu_i \mathbf{V}^{(i)\top})^\top$$

and that

$$\rho_{n,p,m}^2 = \left( \mathbf{r}^\top \frac{\bar{\mathbf{X}}_m}{\|\bar{\mathbf{X}}_m\|} \right)^2 = \frac{\left( \frac{1}{m} \sum_{i=1}^m X_1^{(i)} \right)^2}{\left( \frac{1}{m} \sum_{i=1}^m X_1^{(i)} \right)^2 + \left\| \frac{1}{m} \sum_{i=1}^m \nu_i \mathbf{V}^{(i)} \right\|^2}.$$

Let  $\mathbf{V}'_i$ ,  $i = 1, \dots, n$  be iid uniformly distributed on  $\mathcal{S}^{p-2}$  and independent of  $\mathbf{X}_1, \dots, \mathbf{X}_n$ . Then the following lemma is a consequence of Lemma A4.

**Lemma A5.**

$$\begin{aligned}\rho_{n,p,m}^2 &\stackrel{d}{=} \frac{\left(m^{-1} \sum_{i=1}^m X_1^{(i)}\right)^2}{\left(m^{-1} \sum_{i=1}^m X_1^{(i)}\right)^2 + \left\|m^{-1} \sum_{i=1}^m \nu_i \mathbf{V}_i'\right\|^2} \\ &= \frac{A_{n,p,m}}{A_{n,p,m} + V_{n,p,m}},\end{aligned}\tag{A.3}$$

where

$$A_{n,p,m} = \left(\frac{1}{m} \sum_{i=1}^m X_1^{(i)}\right)^2 \quad \text{and} \quad V_{n,p,m} = \left\|\frac{1}{m} \sum_{i=1}^m \nu_i \mathbf{V}_i'\right\|^2.\tag{A.4}$$

322 The long proofs of Lemmas A6-A8 below are given in Supplementary Material.

324 **Lemma A6.** Let  $m = m_n \rightarrow \infty$  satisfy  $m/n = o(1)$  and  $p = p_n \rightarrow \infty$  satisfy  $(\ln n)^2/p = O(1)$ . Then

(i)

$$\max_{1 \leq i \leq m} \left| p \ln(\sin \Theta_{i:n}) + \ln \frac{n}{i} - \frac{1}{2} \ln \ln \frac{n}{i} \right| = O_p(1),$$

(ii)

$$\max_{1 \leq i \leq m} \left| -\frac{p}{2} \cos^2 \Theta_{i:n} + \ln \frac{n}{i} - \frac{1}{2} \ln \ln \frac{n}{i} \right| = O_p(1),$$

326 where  $\Theta_{1:n} \leq \Theta_{2:n} \leq \dots \leq \Theta_{n:n}$  are the order statistics of  $\Theta_1, \dots, \Theta_n$ .

**Lemma A7.** Suppose that  $p = p_n \rightarrow \infty$  satisfies  $(\ln n)^2/p = O(1)$ .

(i) If  $m = m_n \rightarrow \infty$  satisfies  $m/n \rightarrow 0$ , then

$$-pA_{n,p,m} + 2 \ln \frac{n}{m} - \ln \ln \frac{n}{m} = O_p(1).$$

---

328 (ii) If  $m = m_n \rightarrow \infty$  satisfies  $(\ln m)^3/(\ln n)^2 \rightarrow 0$ , then

$$-pA_{n,p,m} + 2 \ln \frac{n}{m} - \ln \ln \frac{n}{m} - \ln(4\pi) + 2 - \frac{2}{p} \left( \ln \frac{n}{m} \right)^2 = o_p(1).$$

(iii) If  $m = m_n \rightarrow \infty$  satisfies  $m(\ln \ln n)^4/(\ln n)^2 \rightarrow 0$ , then

$$\left( \frac{m}{8} \right)^{1/2} \left\{ -pA_{n,p,m} + 2 \ln \frac{n}{m} - \ln \ln \frac{n}{m} - \ln(4\pi) + 2 - \frac{2}{p} \left( \ln \frac{n}{m} \right)^2 \right\} \xrightarrow{d} N(0, 1).$$

330 **Lemma A8.** Let  $\mathbf{W}_1, \dots, \mathbf{W}_n$  be iid uniformly distributed on  $\mathcal{S}^{p-1}$ . Then

$$\sqrt{\frac{p}{2n^2}} \sum_{1 \leq i \neq \ell \leq n} \langle \mathbf{W}_i, \mathbf{W}_\ell \rangle \xrightarrow{d} N(0, 1) \text{ uniformly as } n \wedge p \rightarrow \infty,$$

where  $\langle \mathbf{W}_i, \mathbf{W}_\ell \rangle$  denotes the inner product of  $\mathbf{W}_i$  and  $\mathbf{W}_\ell$ .

## 332 A.2. Proof of Theorem 1

Theorem 1 is a special case of Theorem A1 below for  $m = 1$ .

334 **Theorem A1.** Let

$$T_{n,p} = (p-1) \ln(\sin \Theta_{m:n}) - K_{n,p},$$

where  $K_{n,p}$  is defined as in (1). Let  $G_m^*(t) = G_m(e^t)$ ,  $t \in \mathbb{R}$ , where  $G_m$

336 denotes the gamma distribution with shape parameter  $m$  and scale parameter

1. Then for fixed  $m = 1, 2, \dots$ ,  $T_{n,p} \xrightarrow{d} G_m^*$  uniformly as  $n \wedge p \rightarrow \infty$ .

*Proof.* We claim that

$$T_{n_\ell, p_\ell} \xrightarrow{d} G_m^* \tag{A.5}$$

for any increasing sequences  $\{n_\ell\}$  and  $\{p_\ell\}$  satisfying  $n_\ell \rightarrow \infty, p_\ell \rightarrow \infty$  and  $(\ln n_\ell)/p_\ell \rightarrow \alpha \in [0, \infty]$  as  $\ell \rightarrow \infty$ . Assume for now that the claim (A.5) holds. To show that  $T_{n,p} \xrightarrow{d} G_m^*$  uniformly as  $n \wedge p \rightarrow \infty$ , suppose to the contrary that  $\limsup_{n \wedge p \rightarrow \infty} \sup_{t \in \mathbb{R}} |\mathbb{P}(T_{n,p} \leq t) - G_m^*(t)| > 0$ . Then there exist an  $\varepsilon > 0$  and a sequence  $\{(n_\ell, p_\ell) : \ell = 1, 2, \dots\}$  such that  $\lim_{\ell \rightarrow \infty} n_\ell \wedge p_\ell = \infty$  and

$$\sup_{t \in \mathbb{R}} |\mathbb{P}(T_{n_\ell, p_\ell} \leq t) - G_m^*(t)| > \varepsilon \text{ for } \ell = 1, 2, \dots \quad (\text{A.6})$$

338 There exists a subsequence  $\{(n_{\ell_k}, p_{\ell_k}) : k = 1, 2, \dots\}$  such that  $(\ln n_{\ell_k})/p_{\ell_k}$  converges to some value  $\alpha \in [0, \infty]$ . Then (A.6) contradicts (A.5), implying  
340 that  $T_{n,p} \xrightarrow{d} G_m^*$  uniformly as  $n \wedge p \rightarrow \infty$ .

We now prove (A.5). For notational simplicity, we will deal only with  
342 the special case where  $n_\ell = \ell$ ,  $\ell = 1, 2, \dots$ . The general case can be treated similarly. Specifically, we show that if  $p = p_n \rightarrow \infty$  satisfies  $(\ln n)/p \rightarrow \alpha \in [0, \infty]$ , then  $T_{n,p} = T_{n,p_n} \xrightarrow{d} G_m^*$ .  
344

Suppose  $p = p_n \rightarrow \infty$  satisfies  $\lim_{n \rightarrow \infty} (\ln n)/p = \alpha \in [0, \infty]$ . For fixed  $m$ , since  $F_p(\Theta_{m:n}) \stackrel{d}{=} U_{m:n}$ , we have by Lemma A3

$$\begin{aligned} \mathbb{P}(nF_p(\Theta_{m:n}) \leq e^t) &= \mathbb{P}(nU_{m:n} \leq e^t) = \mathbb{P}\left(n \frac{S_m}{S_{n+1}} \leq e^t\right) \\ &\longrightarrow \mathbb{P}(S_m \leq e^t) = G_m(e^t) = G_m^*(t). \end{aligned} \quad (\text{A.7})$$

---

For fixed  $t > 0$ , let  $t_n \in [0, 1)$  be such that

$$\frac{p-1}{2} \ln(1 - t_n^2) = \min\{K_{n,p} + t, 0\}.$$

Noting that

$$K_{n,p} = K_{n,p_n} = -(\ln n)(1 + o(1)) \text{ as } n \rightarrow \infty, \quad (\text{A.8})$$

346 we have for large  $n$

$$\frac{p-1}{2} \ln(1 - t_n^2) = K_{n,p} + t < 0. \quad (\text{A.9})$$

By Lemma A2,

$$\left(1 + \frac{1}{(p-3)t_n^2}\right)^{-1} \bar{F}_p(\cos^{-1} t_n) \leq F_p(\cos^{-1} t_n) \leq \bar{F}_p(\cos^{-1} t_n),$$

implying that

$$\begin{aligned} \mathbb{P}(nF_p(\Theta_{m:n}) \leq n\bar{F}_p(\cos^{-1} t_n)) &\geq \mathbb{P}(nF_p(\Theta_{m:n}) \leq nF_p(\cos^{-1} t_n)) \\ &\geq \mathbb{P}\left(nF_p(\Theta_{m:n}) \leq \left(1 + \frac{1}{(p-3)t_n^2}\right)^{-1} n\bar{F}_p(\cos^{-1} t_n)\right). \end{aligned} \quad (\text{A.10})$$

348 Recalling  $\alpha = \lim_{n \rightarrow \infty} (\ln n)/p$ , we claim that for every  $\alpha \in [0, \infty]$ , as

$n \rightarrow \infty$

$$n\bar{F}_p(\cos^{-1} t_n) = e^t + o(1), \quad (\text{A.11})$$

$$pt_n^2 \rightarrow \infty, \quad (\text{A.12})$$

$$\mathbb{P}(\cos \Theta_{m:n} \leq -t_n) \rightarrow 0. \quad (\text{A.13})$$

By (A.7), (A.10), (A.11) and (A.12),

$$P(\cos \Theta_{m:n} \geq t_n) = P(nF_p(\Theta_{m:n}) \leq nF_p(\cos^{-1} t_n)) \rightarrow G_m^*(t). \quad (\text{A.14})$$

Furthermore,

$$\begin{aligned} P(T_{n,p} \leq t) &= P\left(\frac{p-1}{2} \ln(1 - \cos^2 \Theta_{m:n}) - K_{n,p} \leq t\right) \\ &= P(\cos^2 \Theta_{m:n} \geq t_n^2) \quad (\text{by (A.9)}) \\ &= P(\cos \Theta_{m:n} \geq t_n) + P(\cos \Theta_{m:n} \leq -t_n) \\ &\rightarrow G_m^*(t) \quad (\text{by (A.13) and (A.14)}). \end{aligned}$$

It remains to establish (A.11)-(A.13). Note that by Sterling's formula (see e.g. Tricomi and Erdélyi (1951)),

$$\frac{\Gamma(p/2)}{\Gamma((p-1)/2)} = \sqrt{\frac{p}{2}} \left(1 + O\left(\frac{1}{p}\right)\right) \quad \text{as } p \rightarrow \infty. \quad (\text{A.15})$$

We have

$$\begin{aligned} \ln(n\bar{F}_p(\cos^{-1} t_n)) &= \ln\left\{\frac{n}{\sqrt{\pi}} \frac{\Gamma(p/2)}{\Gamma((p-1)/2)} \left(\frac{(1-t_n^2)^{p-1}}{(p-1)^2 t_n^2}\right)^{1/2}\right\} \quad (\text{by (A.2)}) \\ &= \ln\left\{n \left(\frac{(1-t_n^2)^{p-1}}{2\pi p t_n^2}\right)^{1/2}\right\} + O\left(\frac{1}{p}\right) \quad (\text{by (A.15)}) \\ &= \frac{p-1}{2} \ln(1-t_n^2) + \ln n - \frac{1}{2} \ln(pt_n^2) - \frac{1}{2} \ln(2\pi) + O\left(\frac{1}{p}\right) \\ &= K_{n,p} + t + \ln n - \frac{1}{2} \ln(pt_n^2) - \frac{1}{2} \ln(2\pi) + O\left(\frac{1}{p}\right) \quad (\text{by (A.9)}). \end{aligned} \quad (\text{A.16})$$



By (A.8) and (A.9),

$$\ln(1 - t_n^2) = -\frac{2 \ln n}{p}(1 + o(1)), \quad (\text{A.17})$$

implying that

$$t_n \rightarrow (1 - e^{-2\alpha})^{1/2}, \quad (\text{A.18})$$

350 where  $\lim_{n \rightarrow \infty} (\ln n)/p = \alpha \in [0, \infty]$  and  $e^{-\infty} := 0$ .

If  $\alpha = 0$ , we have  $t_n \rightarrow 0^+$ , so that by (A.17)

$$t_n^2 = \frac{2 \ln n}{p}(1 + o(1)), \quad (\text{A.19})$$

from which it follows that  $\ln(pt_n^2) = \ln(2 \ln n) + o(1)$ . By the definition of  $K_{n,p}$ , we have  $K_{n,p} = -\ln n + (\ln \ln n)/2 + \ln(4\pi)/2 + o(1)$ , so that  $K_{n,p} + \ln n - \ln(pt_n^2)/2 - \ln(2\pi)/2 = o(1)$ , which together with (A.16) establishes (A.11) for  $\alpha = 0$ . If  $0 < \alpha < \infty$ , we have  $t_n^2 = 1 - e^{-2\alpha} + o(1)$  (by (A.18)) and  $\ln(pt_n^2) = \ln \ln n - \ln \alpha + \ln(1 - e^{-2\alpha}) + o(1)$ , so that  $K_{n,p} + \ln n - \ln(pt_n^2)/2 - \ln(2\pi)/2 = o(1)$ , which together with (A.16) establishes (A.11) for  $0 < \alpha < \infty$ . If  $\alpha = \infty$ , we have  $t_n \rightarrow 1^-$ , so that by the definition of

$K_{n,p}$ ,

$$\begin{aligned} & K_{n,p} + \ln n - \frac{1}{2} \ln(pt_n^2) - \frac{1}{2} \ln(2\pi) \\ &= -\ln n + \frac{1}{2} \ln \ln n - \frac{1}{2} \ln \left( \frac{2 \ln n}{p} \right) + \frac{1}{2} \ln(4\pi) + \ln n - \frac{1}{2} \ln p - \frac{1}{2} \ln(2\pi) + o(1) \\ &= o(1), \end{aligned}$$

---

which together with (A.16) establishes (A.11) for  $\alpha = \infty$ .

352

Next, (A.19) holds for  $\alpha = 0$ , which implies (A.12). For  $0 < \alpha \leq \infty$ , it  
354 follows from (A.18) that  $t_n \rightarrow (1 - e^{-2\alpha})^{1/2} > 0$ , which implies (A.12).

Finally, to prove (A.13), note that

$$P(\cos \Theta_{m:n} \leq -t_n) \leq P(\Theta_{m:n} \geq \pi/2) = P(B(n, 1/2) < m) \rightarrow 0,$$

356 where  $B(n, 1/2)$  denotes a binomial random variable with parameters  $n$  and  
1/2 (success probability). This establishes (A.13) and completes the proof  
358 of Theorem A1.  $\square$

### A.3. Proofs of Theorems 2-3 and Corollary 1

360 We first show that if  $m = m_n \rightarrow \infty$  satisfies  $m/n \rightarrow 0$  and  $p = p_n \rightarrow \infty$   
satisfies  $(\ln n)^2/p \rightarrow 0$ , then

$$m\sqrt{\frac{p}{2}} \left( V_{n,p,m} - \frac{1}{m} \right) \xrightarrow{d} N(0, 1), \quad (\text{A.20})$$

362 where  $V_{n,p,m} = \left\| \frac{1}{m} \sum_{i=1}^m \nu_i \mathbf{V}'_i \right\|^2$  with  $\nu_i^2 = 1 - \cos^2 \Theta_{i:n}$ , and  $\mathbf{V}'_1, \dots, \mathbf{V}'_m$   
are iid uniformly distributed on  $\mathcal{S}^{p-2}$ , and  $(\mathbf{V}'_1, \dots, \mathbf{V}'_m)$  is independent of  
364  $(\nu_1, \dots, \nu_m)$ .

We have

$$\begin{aligned}
 V_{n,p,m} &= \frac{1}{m^2} \sum_{i=1}^m \nu_i^2 \|\mathbf{V}'_i\|^2 + \frac{1}{m^2} \sum_{1 \leq i \neq \ell \leq m} \nu_i \nu_\ell \langle \mathbf{V}'_i, \mathbf{V}'_\ell \rangle \\
 &= \frac{1}{m} + \frac{1}{m^2} \sum_{i=1}^m (\nu_i^2 - 1) + \frac{1}{m^2} \sum_{1 \leq i \neq \ell \leq m} \{1 + (\nu_i \nu_\ell - 1)\} \langle \mathbf{V}'_i, \mathbf{V}'_\ell \rangle \\
 &= \frac{1}{m} + V'_{1,n} + V'_{2,n} + V'_{3,n},
 \end{aligned} \tag{A.21}$$

where

$$\begin{aligned}
 V'_{1,n} &= \frac{1}{m^2} \sum_{i=1}^m (\nu_i^2 - 1) = -\frac{1}{m^2} \sum_{i=1}^m \cos^2 \Theta_{i:n}, \\
 V'_{2,n} &= \frac{1}{m^2} \sum_{1 \leq i \neq \ell \leq m} \langle \mathbf{V}'_i, \mathbf{V}'_\ell \rangle, \\
 V'_{3,n} &= \frac{1}{m^2} \sum_{1 \leq i \neq \ell \leq m} (\nu_i \nu_\ell - 1) \langle \mathbf{V}'_i, \mathbf{V}'_\ell \rangle.
 \end{aligned}$$

By Lemma A8, we have

$$m \sqrt{\frac{p}{2}} V'_{2,n} \xrightarrow{d} N(0, 1). \tag{A.22}$$

366 It remains to prove

$$mp^{1/2} V'_{i,n} = o_p(1), \quad i = 1, 3. \tag{A.23}$$

By Lemma A6(ii),

$$\max_{1 \leq i \leq m} \cos^2 \Theta_{i:n} = O_p \left( \frac{\ln n}{p} \right),$$

368 implying that  $mp^{1/2} V'_{1,n} = O_p \left( \frac{\ln n}{p^{1/2}} \right) = o_p(1)$ . To show  $mp^{1/2} V'_{3,n} = o_p(1)$ ,

note that  $(\nu_1, \dots, \nu_m)$  is independent of  $(\mathbf{V}'_1, \dots, \mathbf{V}'_m)$  and  $E[\langle \mathbf{V}'_i, \mathbf{V}'_\ell \rangle \langle \mathbf{V}'_{i'}, \mathbf{V}'_{\ell'} \rangle] =$

0 if  $i \neq \ell$ ,  $i' \neq \ell'$  and  $\{i, \ell\} \neq \{i', \ell'\}$ . Also, for  $i \neq \ell$ ,  $E\langle \mathbf{V}'_i, \mathbf{V}'_\ell \rangle^2 = \int_0^\pi \cos^2(\theta) dF_{p-1}(\theta) = \frac{1}{p-1}$ , where  $F_p$  is defined as in (A.1). We have

$$\begin{aligned} EV_{3,n}'^2 &= \frac{2}{m^4} \sum_{1 \leq i \neq \ell \leq m} E[(\nu_i \nu_\ell - 1)^2] E\langle \mathbf{V}'_i, \mathbf{V}'_\ell \rangle^2 \\ &= \frac{2}{m^4} \sum_{1 \leq i \neq \ell \leq m} E[(\nu_i \nu_\ell - 1)^2] \frac{1}{p-1} \\ &= o\left(\frac{1}{m^2 p}\right), \end{aligned} \quad (\text{A.24})$$

since  $|\nu_i| \leq 1$  and  $\nu_i \nu_\ell - 1 \rightarrow 0$  in probability uniformly in  $1 \leq i \neq \ell \leq m$ .

It follows from (A.24) that  $mp^{1/2}V_{3,n}' = o_p(1)$ . This proves (A.23) and

completes the proof of (A.20).

**Proof of Theorem 2.** Since by (A.3)  $\rho_{n,p,m}^2 \stackrel{d}{=} \frac{A_{n,p,m}}{A_{n,p,m} + V_{n,p,m}}$ , we have

$$\rho_{n,p,m}^2 - \frac{\beta_{n,p,m}}{1 + \beta_{n,p,m}} \stackrel{d}{=} \frac{A_{n,p,m} - \beta_{n,p,m}/m}{(A_{n,p,m} + V_{n,p,m})(1 + \beta_{n,p,m})} + \frac{(1/m - V_{n,p,m})\beta_{n,p,m}}{(A_{n,p,m} + V_{n,p,m})(1 + \beta_{n,p,m})}. \quad (\text{A.25})$$

Since  $\beta_{n,p,m} = \frac{m}{p} \{2 \ln \frac{n}{m} - \ln \ln \frac{n}{m} - \ln(4\pi) + 2\}$ , it follows from Lemma

A7(i) and (A.20) that

$$p(A_{n,p,m} - \frac{1}{m}\beta_{n,p,m}) = O_p(1), \quad mV_{n,p,m} = 1 + o_p(1), \quad p\beta_{n,p,m}V_{n,p,m} = (2 + o_p(1)) \ln \left(\frac{n}{m}\right).$$

Thus,

$$\begin{aligned} \frac{A_{n,p,m} - \beta_{n,p,m}/m}{(A_{n,p,m} + V_{n,p,m})(1 + \beta_{n,p,m})} &= \frac{p(A_{n,p,m} - \beta_{n,p,m}/m)}{(p\beta_{n,p,m}A_{n,p,m} + p\beta_{n,p,m}V_{n,p,m})} \frac{\beta_{n,p,m}}{(1 + \beta_{n,p,m})} = o_p(1) \frac{\beta_{n,p,m}}{(1 + \beta_{n,p,m})}, \\ \frac{(1/m - V_{n,p,m})\beta_{n,p,m}}{(A_{n,p,m} + V_{n,p,m})(1 + \beta_{n,p,m})} &= \frac{(1 - mV_{n,p,m})}{(mA_{n,p,m} + mV_{n,p,m})} \frac{\beta_{n,p,m}}{(1 + \beta_{n,p,m})} = o_p(1) \frac{\beta_{n,p,m}}{(1 + \beta_{n,p,m})}. \end{aligned}$$

We have by (A.25),

$$\rho_{n,p,m}^2 = \frac{\beta_{n,p,m}}{1 + \beta_{n,p,m}}(1 + o_p(1)).$$

The proof is complete.  $\square$

380

**Proof of Theorem 3.** By (A.21)-(A.23),

$$\begin{aligned} m\sqrt{\frac{p}{2}} \left( V_{n,p,m} - \frac{1}{m} \right) &= m\sqrt{\frac{p}{2}} (V'_{1,n} + V'_{2,n} + V'_{3,n}) \\ &= m\sqrt{\frac{p}{2}} V'_{2,n} + o_p(1). \end{aligned} \quad (\text{A.26})$$

382 Let

$$\begin{aligned} Z_{1,n} &= p\sqrt{\frac{m}{8}} \left( A_{n,p,m} - \frac{1}{m}\beta_{n,p,m} + \frac{2}{p^2} \left( \ln \frac{n}{m} \right)^2 \right), \\ Z_{2,n} &= m\sqrt{\frac{p}{2}} V'_{2,n}, \\ \gamma_n &= (A_{n,p,m} + V_{n,p,m})(1 + \beta_{n,p,m}). \end{aligned}$$

We have by (A.25) and (A.26)

$$\begin{aligned} &\rho_{n,p,m}^2 - \frac{\beta_{n,p,m}}{1 + \beta_{n,p,m}} \\ &\stackrel{d}{=} \gamma_n^{-1} \left\{ \frac{1}{p\sqrt{m/8}} Z_{1,n} - \frac{\beta_{n,p,m}}{m\sqrt{p/2}} m\sqrt{\frac{p}{2}} \left( V_{n,p,m} - \frac{1}{m} \right) \right\} - \gamma_n^{-1} \frac{2}{p^2} \left( \ln \frac{n}{m} \right)^2 \\ &= \gamma_n^{-1} \left\{ \sqrt{\frac{8}{mp^2}} Z_{1,n} - \sqrt{\frac{2}{m^2 p}} \beta_{n,p,m} (Z_{2,n} + o_p(1)) \right\} - \gamma_n^{-1} \frac{2}{p^2} \left( \ln \frac{n}{m} \right)^2 \\ &= \gamma_n^{-1} \left( \frac{8}{mp^2} + \frac{2}{m^2 p} \beta_{n,p,m}^2 \right)^{1/2} \{ c_{1,n} Z_{1,n} + c_{2,n} (Z_{2,n} + o_p(1)) \} - \gamma_n^{-1} \frac{2}{p^2} \left( \ln \frac{n}{m} \right)^2, \end{aligned} \quad (\text{A.27})$$

384 where

$$\begin{aligned} c_{1,n} &= \sqrt{\frac{8}{mp^2}} \left( \frac{8}{mp^2} + \frac{2}{m^2p} \beta_{n,p,m}^2 \right)^{-1/2}, \\ c_{2,n} &= -\sqrt{\frac{2}{m^2p}} \beta_{n,p,m} \left( \frac{8}{mp^2} + \frac{2}{m^2p} \beta_{n,p,m}^2 \right)^{-1/2}. \end{aligned}$$

Since  $\rho_{n,p,m}^2 \stackrel{d}{=} A_{n,p,m}/(A_{n,p,m} + V_{n,p,m})$ , we have by Theorem 2

$$\frac{A_{n,p,m}}{A_{n,p,m} + V_{n,p,m}} = \frac{\beta_{n,p,m}}{1 + \beta_{n,p,m}}(1 + o_p(1)). \quad (\text{A.28})$$

386 It follows from Lemma A7(i) and  $(p/m)\beta_{n,p,m} = 2 \ln \frac{n}{m}(1 + o(1))$  that

$$\frac{mA_{n,p,m}}{\beta_{n,p,m}} = \frac{pA_{n,p,m}}{(p/m)\beta_{n,p,m}} = 1 + o_p(1). \quad (\text{A.29})$$

So we have

$$\begin{aligned} \gamma_n \left( \frac{8}{mp^2} + \frac{2}{m^2p} \beta_{n,p,m}^2 \right)^{-1/2} &= \frac{pm}{\sqrt{8m + 2p\beta_{n,p,m}^2}} (A_{n,p,m} + V_{n,p,m})(1 + \beta_{n,p,m}) \\ &= \frac{pmA_{n,p,m}}{\sqrt{8m + 2p\beta_{n,p,m}^2}} \frac{A_{n,p,m} + V_{n,p,m}}{A_{n,p,m}} (1 + \beta_{n,p,m}) \\ &= \frac{pmA_{n,p,m}/\beta_{n,p,m}}{\sqrt{8m + 2p\beta_{n,p,m}^2}} (1 + \beta_{n,p,m})^2 (1 + o_p(1)) \quad (\text{by (A.28)}) \\ &= \frac{p}{\sqrt{8m + 2p\beta_{n,p,m}^2}} (1 + \beta_{n,p,m})^2 (1 + o_p(1)) \quad (\text{by (A.29)}) \\ &= \alpha_{n,p,m} (1 + o_p(1)), \end{aligned} \quad (\text{A.30})$$

388 where  $\alpha_{n,p,m} = p (8m + 2p\beta_{n,p,m}^2)^{-1/2} (1 + \beta_{n,p,m})^2$ .

Also,

$$\begin{aligned}
 0 &< \frac{2}{p^2} \left( \ln \frac{n}{m} \right)^2 \left( \frac{8}{mp^2} + \frac{2}{m^2 p} \beta_{n,p,m}^2 \right)^{-1/2} \\
 &\leq \frac{2}{p^2} \left( \ln \frac{n}{m} \right)^2 \left( \frac{2}{m^2 p} \beta_{n,p,m}^2 \right)^{-1/2} \\
 &= \frac{2}{p^2} \left( \ln \frac{n}{m} \right)^2 \left\{ \frac{2}{p^3} \left( \frac{p}{m} \beta_{n,p,m} \right)^2 \right\}^{-1/2} \\
 &= \sqrt{\frac{2}{p}} \left( \ln \frac{n}{m} \right)^2 \left( 2 \ln \frac{n}{m} (1 + o(1)) \right)^{-1} \\
 &= \frac{1}{\sqrt{2p}} \ln \frac{n}{m} (1 + o(1)) = o(1),
 \end{aligned}$$

390 which together with (A.30) implies that

$$\begin{aligned}
 &\frac{\alpha_{n,p,m}}{\gamma_n} \frac{2}{p^2} \left( \ln \frac{n}{m} \right)^2 \\
 &= \left\{ \frac{\alpha_{n,p,m}}{\gamma_n} \left( \frac{8}{mp^2} + \frac{2}{m^2 p} \beta_{n,p,m}^2 \right)^{1/2} \right\} \left\{ \frac{2}{p^2} \left( \ln \frac{n}{m} \right)^2 \left( \frac{8}{mp^2} + \frac{2}{m^2 p} \beta_{n,p,m}^2 \right)^{-1/2} \right\} \\
 &= (1 + o_p(1)) o(1) = o_p(1). \tag{A.31}
 \end{aligned}$$

It follows from (A.27), (A.30), and (A.31) that

$$\begin{aligned}
 &\alpha_{n,p,m} \left( \rho_{n,p,m}^2 - \frac{\beta_{n,p,m}}{1 + \beta_{n,p,m}} \right) \\
 &\stackrel{d}{=} \frac{\alpha_{n,p,m}}{\gamma_n} \left( \frac{8}{mp^2} + \frac{2}{m^2 p} \beta_{n,p,m}^2 \right)^{1/2} \{c_{1,n} Z_{1,n} + c_{2,n} Z_{2,n} (1 + o_p(1))\} - \frac{\alpha_{n,p,m}}{\gamma_n} \frac{2}{p^2} \left( \ln \frac{n}{m} \right)^2 \\
 &= (1 + o_p(1)) \{c_{1,n} Z_{1,n} + c_{2,n} Z_{2,n} (1 + o_p(1))\} + o_p(1). \tag{A.32}
 \end{aligned}$$

392 Note that  $c_{1,n}$  and  $c_{2,n}$  are constants (depending on  $n, p_n, m_n$ ), which satisfy

$c_{1,n}^2 + c_{2,n}^2 = 1$ . By Lemma A7(iii),

$$-Z_{1,n} = \sqrt{\frac{m}{8}} \left\{ -p A_{n,p,m} + 2 \ln \frac{n}{m} - \ln \ln \frac{n}{m} - \ln(4\pi) + 2 - \frac{2}{p} \left( \ln \frac{n}{m} \right)^2 \right\} \xrightarrow{d} N(0, 1).$$

394 By (A.22),  $Z_{2,n} \xrightarrow{d} N(0, 1)$ . Note that  $Z_{1,n}$  and  $Z_{2,n}$  are independent (since  $A_{n,p,m}$  and  $V'_{2,n}$  are independent). We have

$$c_{1,n}Z_{1,n} + c_{2,n}Z_{2,n} \xrightarrow{d} N(0, 1),$$

396 which together with (A.32) implies that

$$\alpha_{n,p,m} \left( \rho_{n,p,m}^2 - \frac{\beta_{n,p,m}}{1 + \beta_{n,p,m}} \right) \xrightarrow{d} N(0, 1).$$

The proof is complete.

398 **Proof of Corollary 1.** Part (i) follows immediately from Theorem 2. To prove part (ii), we have by part (i) and Theorem 3 that

$$\begin{aligned} & 2\alpha_{n,p,m} \sqrt{\frac{\beta_{n,p,m}}{1 + \beta_{n,p,m}}} \left( \rho_{n,p,m} - \sqrt{\frac{\beta_{n,p,m}}{1 + \beta_{n,p,m}}} \right) \\ &= \frac{2\sqrt{\frac{\beta_{n,p,m}}{1 + \beta_{n,p,m}}}}{\rho_{n,p,m} + \sqrt{\frac{\beta_{n,p,m}}{1 + \beta_{n,p,m}}}} \alpha_{n,p,m} \left( \rho_{n,p,m}^2 - \frac{\beta_{n,p,m}}{1 + \beta_{n,p,m}} \right) \xrightarrow{d} N(0, 1), \end{aligned}$$

400 completing the proof. □

## References

- 402 Cai, T. T., Fan, J., and Jiang, T. (2013). Distributions of angles in random packing on spheres. *Journal of Machine Learning Research* **14**, 1837–1864.
- 404 Cai, T. T. and Jiang, T. (2011). Limiting laws of coherence of random matrices with applications to testing covariance structure and construction of compressed sensing matrices. *Annals of Statistics* **39**, 1496–1525.
- 406



## REFERENCES

- Cai, T. T. and Jiang, T. (2012). Phase transition in limiting distributions of coherence of  
408 high-dimensional random matrices. *Journal of Multivariate Analysis* **107**, 24–39.
- Fan, J., Guo, S., and Hao, N. (2012). Variance estimation using refitted cross-validation in  
410 ultrahigh dimensional regression. *Journal of the Royal Statistical Society: Series B* **74**,  
37–65.
- 412 Fan, J., Shao, Q. M., and Zhou, W. X. (2018). Are discoveries spurious? Distributions of  
maximum spurious correlations and their applications. *Annals of Statistics* **46**, 989–1017.
- 414 Henderson, R. (2013). Avoiding the pitfalls of single particle cryo-electron microscopy: Einstein  
from noise. *Proceedings of the National Academy of Sciences U.S.A.* **110**, 18037–18041.
- 416 Karlin, S. and Taylor, H. M. (1975). *A First Course in Stochastic Processes*. Academic Press.
- Lai, T. L., Wang, S.-H., Yao, Y.-C., Chung, S.-C., Chang, W.-H., and Tu, I.-P. (2020). *Cryo-EM:*  
418 *Breakthroughs in chemistry, structural biology, and statistical underpinnings*. Technical  
Report, Center for Innovative Study Design, Stanford University.
- 420 Liao, M., Cao, E., Julius, D., and Cheng, Y. (2013). Structure of the TRPV1 ion channel  
determined by electron cryo-microscopy. *Nature* **504**, 107–112.
- 422 Stewart, A. and Grigorieff, N. (2004). Noise bias in the refinement of structures derived from  
single particles. *Ultramicroscopy* **102**, 67–84.
- 424 Tricomi, F. G. and Erdélyi, A. (1951). The asymptotic expansion of a ratio of gamma functions.  
*Pacific Journal of Mathematics* **1**, 133–142.

---

## REFERENCES

- 426 Yan, C., Hang, J., Wan, R., Huang, M., Wong, C. C., and Shi, Y. (2015). Structure of a yeast spliceosome at 3.6-angstrom resolution. *Science* **349**, 1182–1191.